Note that for $p = \frac{1}{2}$ we get the Miller relationship for the barrier position, while $p = 1$ gets us the Marcus relationship for the barrier position (eq 31, rhs). It is interesting that two examples of double-minima reaction coordinates have been examined, and it appears that $p > 1$ gives a better account of the nonlinearity seen for $g_{1a}(X)$ vs. X than $p \leq 1$.[22a,25] It is too early to tell whether specific values of p, or ranges of p, will correspond to the number of maxima and minima along the reaction coordinate, but it is clear that a single value of p will not be universal. Since values larger than one and less than one have been found, it would appear that the Marcus relationship for the barrier position (eq 31, rhs), corresponding to $p = 1$, may be a comfortable, although somewhat imprecise, compromise.

VI. Conclusions

Miller has previously developed a simple and remarkably successful relationship for predicting the barrier position in terms of $\Delta E^{\ddagger}$ and ΔE, and it has been found that at least one new condition is necessary for obtaining Miller's equation. A sufficient condition has been identified and is termed a scaled symmetry relationship. The general class of barrier functions (nonspline) which exhibit the scaled symmetry relationship has been defined. All of them lead to the Marcus relationship for the *barrier height*, and special cases lead to the Marcus or Miller relationships for the *barrier position* along the reaction coordinate. The scaled symmetry relationship follows from limiting the expansion of the reaction coordinate to second-order terms in suitable functions and forms a general basis for extending Marcus-like equations to *all* one-step reactions, including electron, proton, and group transfers, pericyclic processes, additions, fragmentations, cheletropic reactions, conformational equilibria, isomerizations, and so forth. The fundamental basis of the scaled symmetry relationship is undergoing examination.[22,25,27]

Supplementary Material Available: Arc-length minimization for cubic and quartic polynomials (Table I*), arc length minimization criteria (Appendix I*), and derivation of functions satisfying the scaled symmetry relationship (Appendix II*) (13 pages). Ordering information is given on any current masthead page.

(27) (a) J. R. Murdoch, *J. Am. Chem. Soc.*, **104**, 588 (1982); (b) J. R. Murdoch and D. E. Magnoli, *ibid.*, **104**, 2782 (1982); (c) J. R. Murdoch and D. E. Magnoli, *ibid.*, **104**, 3792 (1982); (d) J. R. Murdoch, *ibid.*, **105**, 2159 (1983). (e) J. R. Murdoch and D. E. Magnoli, *ibid.*, **104**, 3792 (1982). (f) J. R. Murdoch and D. E. Magnoli, *J. Chem. Phys.*, **77**, 4558 (1982).

Intrinsic Barriers in Nucleophilic Displacements. A General Model for Intrinsic Nucleophilicity toward Methyl Centers

Mark J. Pellerite and John I. Brauman*

Contribution from the Department of Chemistry, Stanford University, Stanford, California 94305. Received May 3, 1982

Abstract: The applicability of the Marcus rate–equilibrium formalism to the double-minimum potential energy surface for gas-phase S_N2 reactions is proposed and used to develop a model for intrinsic nucleophilicity toward methyl centers. The key quantities in this model are the energy barriers to degenerate reactions of the form $X^- \cdot CH_3X \rightarrow XCH_3 \cdot X^-$, in which the reacting species are ion–molecule cluster intermediates. Available experimental and theoretical data corroborate several of the model's predictions. A new structure–nucleophilicity correlation is proposed, involving methyl cation affinities. The model suggests that delocalization effects do not greatly influence nucleophile reactivity.

How readily do the species X and Y participate in a nucleophilic displacement reaction such as eq 1? The concept of nucleo-

$$X^- + CH_3Y \rightarrow Y^- + CH_3X \qquad (1)$$
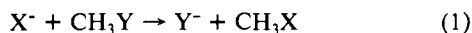
philicity in S_N2 reactions of aliphatic systems has been a cornerstone of organic chemistry ever since the early kinetic and stereochemical investigations of Ingold and co-workers.[1] Some indication of this can be found in the considerable body of work devoted to the quantitative description of nucleophilicity. Results of this effort include linear free energy relationships such as the Swain–Scott[2a] and Edwards[2b] equations and the general treatment of Hudson.[2c] However, a completely satisfactory and unambiguous scheme for this quantification has yet to be presented, and the success and scope of the above treatments are limited. Part of

the difficulty arises from solvent effects, as even relative reactivities in S_N2 reactions can be solvent dependent.[3] This factor renders separation of intrinsic and solvent effects on the basis of solution-phase data difficult if not impossible. Also, nucleophilicity is inherently a kinetic property; according to such rate–equilibrium treatments as the Bell–Evans–Polanyi principle,[4] reaction rates can be affected by thermodynamics. Thus, a complete description of nucleophilicity requires some means of compensating for any thermodynamic driving force. In general, this feature has not been included in past efforts.[5]

(1) Ingold, C. K. "Structure and Mechanism in Organic Chemistry"; Cornell University Press: Ithaca, New York, 1969; p 422 ff.
(2) (a) Swain, C. G.; Scott, C. C. *J. Am. Chem. Soc.* **1953**, *75*, 141. (b) Edwards, J. D. *Ibid.* **1956**, *78*, 1819. (c) Hudson, R. F. *Chimia* **1962**, *16*, 173.

(3) Parker, A. J. *Chem. Rev.* **1969**, *69*, 1.
(4) (a) Bell, R. P. *Proc. R. Soc. London, Ser. A* **1936**, *A154*, 414. (b) Evans, M. G.; Polanyi, M. *Trans. Faraday Soc.* **1938**, *34*, 11 and references cited therein.
(5) However, a treatment of S_N2 reactions in solution has appeared recently (Albery, W. J.; Kreevoy, M. M. *Adv. Phys. Org. Chem.* **1978**, *16*, 87) in which the kinetic–thermodynamic separation has been accomplished by using the Marcus equation, as we do here for the analogous gas-phase process. However, this work does not allow separation of solvent and intrinsic effects.

Table I. Experimental Rate Constants, Efficiencies, and Calculated Thermochemical Data for Gas-Phase S_N2 Reactions

reaction	k^a	$k_{coll}{}^{a,b}$	efficiency^c	k, other work^a	$\Delta H°,{}^d$ kcal/mol
$CH_3O^- + CH_3Cl \rightarrow Cl^- + CH_3OCH_3$	6.0 ± 0.6	19.9	0.30 ± 0.03	4.9,^{e} 16,^{f} 13^g	−42
$t\text{-BuO}^- + CH_3Cl \rightarrow Cl^- + t\text{-BuOCH}_3$	1.6 ± 0.2	15.9	0.10 ± 0.01	8.0^f	−35
$HCC^- + CH_3Cl \rightarrow Cl^- + HCCCH_3$	0.52 ± 0.07	21.4	0.024 ± 0.003	1.3^g	−51
$F^- + CH_3Cl \rightarrow Cl^- + CH_3F$	5.8 ± 0.3	23.4	0.25 ± 0.01	8.0,^{e} 18,^{f} 19^g	−28
$CD_3S^- + CH_3Cl \rightarrow Cl^- + CD_3SCH_3$	0.52 ± 0.1	17.6	0.03 ± 0.006	0.78,^{e} 1.1	−29
$CH_3O^- + CH_3Br \rightarrow Br^- + CH_3OCH_3$	7.3 ± 0.2	18.0	0.40 ± 0.01	7.2,^{e} 11^g	−49
$t\text{-BuO}^- + CH_3Br \rightarrow Br^- + t\text{-BuOCH}_3$	4.1 ± 0.5	13.5	0.30 ± 0.04		−43
$HCC^- + CH_3Br \rightarrow Br^- + HCCCH_3$	3.1 ± 0.30	19.6	0.16 ± 0.02	5.2^g	−59
$CH_3CO_2{}^- + CH_3Br \rightarrow Br^- + CH_3CO_2CH_3$	0.20 ± 0.04	14.4	0.014 ± 0.003		−17

^{a} Units of 10^{-10} cm^3 molecule^{-1} s^{-1}, measured at $T \approx 313$ K. ^{b} Calculated from ADO theory; see ref 13. ^{c} k/k_{coll}. ^{d} Calculated with data from ref 52 and 53. ^{e} Reference 7. ^{f} Reference 45. ^{g} Reference 37.

$$X^- + CH_3X \underset{k_{-1}}{\overset{k_1}{\rightleftharpoons}} X \cdot CH_3X \underset{k_{-2}}{\overset{k_2}{\rightleftharpoons}} XCH_3 \cdot X^- \underset{k_{-3}}{\overset{k_3}{\rightleftharpoons}} CH_3X + X^-$$
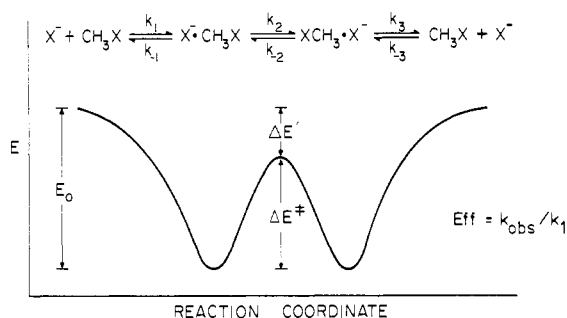
Eff = k_{obs}/k_1

REACTION COORDINATE

Figure 1. Double-minimum potential energy surface for degenerate S_N2 reaction.

The work described in this paper represents one step toward a quantitative picture of nucleophilicity. We propose here a general model, based on an extension of our earlier work, allowing unambiguous description of intrinsic nucleophilicities in gas-phase S_N2 reactions of the form shown in eq 1. It is hoped that an understanding of these reactions in the absence of solvent may help to provide insight into the dynamics of their condensed-phase counterparts.[6]

Available evidence indicates that gas-phase nucleophilic displacements of the form of eq 1 can be interpreted with a double-minimum potential energy reaction coordinate diagram as illustrated in Figure 1 for a degenerate exchange reaction. This model has been discussed in detail by Olmstead and Brauman in an earlier publication.[7] They also proposed a method for evaluating $\Delta E^{\ddagger}$, the central barrier height. Our original work,[8] based on this treatment, proposed applicability of the Marcus rate-equilibrium formalism[9] to $\Delta E^{\ddagger}$ and the ΔE for the elementary transfer step shown in eq 2. The Marcus equation provides a

$$X^- \cdot CH_3Y \rightleftharpoons Y^- \cdot CH_3X \qquad (2)$$
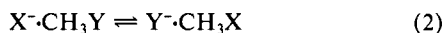
convenient means of separating kinetic and thermodynamic contributions to energy barriers. To illustrate the utility of this concept, we applied the model to several S_N2 reactions involving halides and alkoxides and drew some novel conclusions concerning relative reactivities of these species. However, at that time little evidence was available to support or refute our proposal. This paper details subsequent work on additional systems and examines evidence which indicates that our model may be of general applicability in these reactions.

Experimental Section

Instrumentation. Rate constants were measured with a pulsed ion cyclotron resonance[10] spectrometer equipped with a trapped-ion cell.

Marginal oscillator frequencies were 153.5 or 307 kHz. Total pressures were 10^{-6}–10^{-5} torr, measured with a Varian UHV-24 ionization gauge calibrated for each reactant gas in the 10^{-5}–10^{-4}-torr range against an MKS Baratron capacitance manometer.

Determination of Rate Constants. Primary ions were generated by electron impact on a source gas at pressures of $\sim 10^{-7}$ torr. The ions were scanned over time to check for adequate trapping and the absence of unwanted side reactions, and then a known pressure of reactant gas was added. The pseudo-first-order decay of the reactant ion was recorded, and the rate constant was determined from this trace and the reactant-gas pressure. This procedure was repeated at different reactant-gas pressures and on different days. All reactions were confirmed with double-resonance ion ejection, and the rate constants are reported as the mean and standard deviation of multiple runs. For reactions with rate constants less than $\sim 1 \times 10^{-10}$ cm^3 molecule^{-1} s^{-1}, corrections for nonreactive ion loss were made by using the empirical method developed by Olmstead.[7] Finally, whenever possible, kinetic data for product-ion rise in addition to reactant-ion decay were collected and analyzed. Some of the species studied here cannot be prepared in the gas phase by direct electron impact; hence, in most cases they were generated via proton transfer from their conjugate acids to a base such as F^- or $t\text{-BuO}^-$.

Materials. Dimethyl peroxide (CH_3OOCH_3) was prepared according to the procedure of Hanst and Calvert.[11] All other compounds were obtained commercially and used without further purification, with the exception of phenyl azide, which was purchased as a n-hexane solution. The hexane was removed on a rotary evaporator and the phenyl azide transferred under vacuum into a sample finger for use on the ICR. The IR spectrum of the material thus obtained revealed no significant impurities.

Sources of primary ions were as follows: (ion/precursor/electron energy in eV), $F^-/NF_3/0$–2; $CH_3O^-/CH_3OOCH_3/0$–2; $t\text{-BuO}^-/t\text{-BuOO}$-$t$-Bu/1–3; $CH_3CO_2{}^-/CH_3CO_2COCH_3/0$–3; $CD_3S^-/CD_3SSCD_3/1$–2; $PhN \cdot/PhN_3/0$–2. All other nucleophiles in this study were prepared via proton transfer as mentioned previously.

Results

The relevant experimental and thermochemical data are shown in Tables I and II. Ion–molecule collision rate constants for use in the experimental efficiency calculations were estimated by using Average Dipole Orientation (ADO) theory.[13] Reliability of the measured rate constants is believed to be about ±30%, due primarily to uncertainty in the Baratron readings below 10^{-4} torr. However, relative rate constants, especially those for different ions reacting with a common substrate, should be more reliable than this ($\sim$±10%).
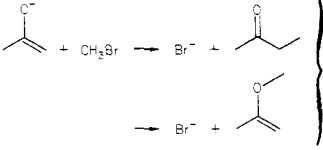
Calculations

RRKM. Since details of the method for estimating $\Delta E^{\ddagger}$ in Figure 1 have been discussed in detail elsewhere,[7,8] a brief treatment suffices here. Furthermore, we do not address the question of applicability of statistical rate theory to ion–molecule processes of this type, except to point out that RRKM calculations

(6) The view that this approach is futile has been expressed recently (Albery, W. J. *Annu. Rev. Phys. Chem.* **1980**, *31*, 227), but as will be seen later, our work shows that barriers in S_N2 reactions cannot be accounted for completely by desolvation effects.

(7) Olmstead, W. N.; Brauman, J. I. *J. Am. Chem. Soc.* **1977**, *99*, 4219.

(8) Pellerite, M. J.; Brauman, J. I. *J. Am. Chem. Soc.* **1980**, *102*, 5993.

(9) Marcus, R. A. *J. Phys. Chem.* **1968**, *72*, 891.

(10) McIver, R. T., Jr. *Rev. Sci. Instrum.* **1978**, *49*, 111 and references cited therein.

(11) Hanst, P. L.; Calvert, J. G. *J. Phys. Chem.* **1959**, *63*, 105.

(12) (a) Olmstead, W. N.; Lev-On, M.; Golden, D. M.; Brauman, J. I. *J. Am. Chem. Soc.* **1977**, *99*, 992. (b) Jasinski, J. M.; Rosenfeld, R. N.; Golden, D. M.; Brauman, J. I. *Ibid.* **1979**, *101*, 2259.

(13) Efficiency is defined as the fraction of collisions resulting in reaction: Eff = k_{obsd}/k_{coll} where k_{coll} is the ion–molecule collision rate constant. For collisions involving polar molecules, k_{coll} may be calculated by using Average Dipole Orientation theory: Su, T.; Bowers, M. T. *Int. J. Mass Spectrom. Ion Phys.* **1973**, *12*, 347.

Table II. Experimental Rate Constants, Efficiencies, and Calculated Thermochemical Data for S_N2 Reactions of Delocalized Nucleophiles

reaction	k^a	Eff^b	$\Delta H°$,^{c} kcal/mol
$CH_3CO_2^- + CH_3Br \rightarrow Br^- + CH_3CO_2CH_3$	0.20 ± 0.04^d	0.014 ± 0.003	-17
$CN^- + CH_3Br \rightarrow Br^- + CH_3CN$ $\Big\}$	0.20^e	0.01	-35
$\qquad\qquad Br^- + CH_3NC$			-21
(enolate structures)			-47
$\quad + CH_3Br \rightarrow Br^- +$ $\Big\}$	1.8 ± 0.02^d	0.12 ± 0.01	
$\rightarrow Br^- +$			-25
$PhN^{-\cdot} + CH_3Br \rightarrow Br^- + Ph\dot{N}CH_3$	0.19 ± 0.03^d	0.015 ± 0.002	-48
$CH_2CN^- + CH_3Br \rightarrow Br^- + CH_3CH_2CN$	2.9 ± 0.5^d	0.18 ± 0.03	-55
$PhCH_2^- + CH_3Cl \rightarrow Cl^- + PhCH_2CH_3$	0.15^f	0.01	-51
$c\text{-}C_5H_5^- + CH_3Br \rightarrow c\text{-}C_5H_5CH_3 + Br^-$			
$PhO^- + CH_3Br \rightarrow PhOCH_3 + Br^-$ $\Big\}$	$\leqslant \sim 0.1^d$		
$CF_3COCH_2^- + CH_3Br \rightarrow (CF_3COCH_2)CH_3 + Br^-$			

^{a} Units of 10^{-10} cm^3 molecule^{-1} s^{-1}, measured at $T \approx 313$ K. ^{b} k/k_{coll}. k_{coll} calculated from ADO theory (ref 13). ^{c} Calculated with data from ref 52 and 53. ^{d} This work. ^{e} Reference 7. ^{f} Reference 45.

have been remarkably successful in describing kinetics of three-body ion–molecule association reactions.[12]

It can be shown[7] that the efficiency[13] of the reaction in Figure 1 depends only on the branching ratio k_2/k_{-1}, where k_2 and k_{-1} represent the unimolecular rate constants for dissociation of the reactants complex into reactant (k_{-1}) and product (k_2) channels.[14] Since the complex lies at lower energy than the reactants, and the pressure in ICR experiments is generally low enough to preclude collisions during the lifetime of the complex, this branching ratio can be calculated by using RRKM theory[15] if we assume the excess internal energy to be randomized rapidly among all of the internal degrees of freedom. To perform this calculation, we need to specify vibrational frequencies, moments of inertia for internal rotors, and external moments for the transition states leading to the reactant and product channels.[16] For all reactions studied here, these parameters were chosen according to methods outlined previously.[8] Once the choices of transition-state parameters are made, the calculated branching ratio depends only on temperature and the energy gap $\Delta E' = E_0 - \Delta E^{\ddagger}$ between the ground vibrational levels of the two transition states. Thus, a determination of $\Delta E^{\ddagger}$ by this method begins with construction of a plot of calculated efficiency vs. $\Delta E'$ for the reaction of interest.[8] The experimental efficiency is fit to this plot and an "experimental" $\Delta E'$ obtained. This can be converted into $\Delta E^{\ddagger}$ provided the well depth E_0 is known (Figure 1). This well depth, ignoring the difference of RT between energy and enthalpy changes, assuming ideal behavior, corresponds to $\Delta H°$ for the clustering of the reactant ion and neutral. These quantities have been measured[17] for several halide–methyl halide association complexes and are generally in the range of 9–10 kcal/mol. As the binding in these complexes is probably mainly electrostatic, we assume for purposes of our calculations that the well depth depends only on the polarizability and dipole moment of the neutral and not on the structure of the ion. The error introduced by this assumption is probably small compared to the error introduced by uncertainties in the RRKM calculations (see below).

Results of the central barrier height determinations for reactions in Table I appear in Table III. The three entries that appear for each reaction correspond to different sets of RRKM input parameters.[8] Vibrational frequencies for several low-frequency modes in the k_2 transition state are not estimated easily for lack

Table III. Potential Surface Data and Marcus Calculations for $X^- + CH_3Y \rightarrow Y^- + CH_3X$

X	Y	model, cm^{-1}	$\Delta E'$, kcal/mol	$\Delta E^{\ddagger}$, kcal/mol	$\Delta E^{\ddagger}_0$, kcal/mol	α	$\Delta E^{\ddagger}_0$-$(X^- + CH_3X)$,^{a} kcal/mol
CH_3O	Cl	100	3.1	5.9	21.4	0.26	33.5
		200	5.6	3.4	18.4	0.21	26.6
		300	7.2	1.8	15.8	0.17	21.5
t-BuO	Cl	100	2.4	6.6	21.4	0.28	32.6
		200	3.9	5.1	19.5	0.26	28.8
		300	4.7	4.3	18.3	0.24	26.4
HCC	Cl	100	0.8	8.2	27.9	0.27	45.5
		200	2.8	6.2	25.4	0.25	40.6
		300	4.2	4.8	23.3	0.23	36.5
F	Cl	100	0.9	8.1	19.6	0.32	29.0
		200	2.1	6.9	18.2	0.31	26.2
		300	3.2	5.8	16.9	0.29	23.6
CD_3S	Cl	100	1.3	7.7	19.1	0.31	28.1
		200	3.0	6.0	17.2	0.29	24.2
		300	4.0	5.0	15.9	0.27	21.6
CH_3O	Br	100	3.9	6.1	24.5	0.25	37.8
		200	6.7	3.3	20.5	0.20	29.2
		300	8.6	1.4	17.2	0.14	23.2
t-BuO	Br	100	4.0	6.0	23.3	0.25	35.4
		200	5.8	4.2	20.9	0.22	30.6
		300	6.8	3.2	19.4	0.20	27.6
HCC	Br	100	2.2	7.8	30.1	0.25	48.9
		200	5.0	5.0	26.2	0.22	41.2
		300	7.0	3.0	23.1	0.18	34.9
CH_3CO_2	Br	100	2.6	7.4	16.6	0.33	21.9
		200	4.8	5.2	14.1	0.30	17.0
		300	6.1	3.9	12.5	0.28	13.8

^{a} Calculated with $\Delta E^{\ddagger}_0(Cl^- + CH_3Cl) = 10.2$ kcal/mol, $\Delta E^{\ddagger}_0$-$(Br^- + CH_3Br) = 11.2$ kcal/mol, determined (see text) with experimental efficiencies from ref 7. The barrier for $Br^- + CH_3Br$ is only approximate.[7] $\Delta E^{\ddagger}_0(Cl^- + CH_3Cl)$ and $\Delta E^{\ddagger}_0(Br^- + CH_3Br)$ varied little as a function of model; hence the results from the 200-cm^{-1} model were used in all calculations.

of suitable models. Thus, three sets of calculations were performed by using different assumed values for these frequencies.

Marcus Theory. Equation 3 shows the potential energy form of the Marcus equations.[9,18] Equation 3a expresses the energy

$$\Delta E^{\ddagger} = [(\Delta E)^2/16\Delta E^{\ddagger}_0] + \Delta E^{\ddagger}_0 + \tfrac{1}{2}\Delta E \qquad (3a)$$

$$\alpha = (\Delta E/8\Delta E^{\ddagger}_0) + \tfrac{1}{2} \qquad (3b)$$

(14) Although the model is illustrated here for a degenerate reaction, the extension to the more general, nonthermoneutral case is straightforward (ref 7).

(15) (a) Forst, W. "Theory of Unimolecular Reactions"; Academic Press: New York, 1973. (b) Robinson, P. J.; Holbrook, K. A. "Unimolecular Reactions"; Wiley-Interscience: New York, 1972.

(16) All dependence on the properties of the intermediate complex vanishes since we are considering only a branching ratio.

(17) (a) Dougherty, R. C.; Dalton, J.; Roberts, J. D. *Org. Mass Spectrom.* **1974**, *8*, 77. (b) Dougherty, R. C.; Roberts, J. D. *Ibid.* **1974**, *8*, 81. (c) Dougherty, R. C. *Ibid.* **1974**, *8*, 85.

barrier $\Delta E^{\ddagger}$ for an elementary reaction in terms of the exo- or endothermicity ΔE and an "intrinsic" barrier, which is the barrier height at $\Delta E = 0$. The fractional position of the transition state along the reaction coordinate, α, is given by eq 3b. The intrinsic barrier for the general transfer reaction AX + B → BX + A can be regarded[9] as the mean of the barriers for the degenerate exchanges A + AX → AX + A and B + BX → BX + B. This is a key feature of the Marcus framework, and one that plays a crucial role in our later discussion of intrinsic nucleophilicities.

Marcus theory has thus far been applied to electron-[19] and proton-transfer[20] reactions in solution, S_N2 reactions in solution,[5,21] a few gas-phase atom transfers,[9] and well depths for hydrogen-bonded gaseous ion–molecule complexes.[22] The theoretical foundation of its applicability to electron-transfer processes is beyond dispute;[23] that is not the case for transfer of heavier particles, however, as the equation was derived originally[24] for intersecting parabolic potential surfaces in the zero-overlap approximation. For heavier particle transfer, the quartic potential of le Noble et al.[25] is certainly a better description of the reaction coordinate in such reactions as proton transfer or nucleophilic displacement (methyl transfer[5]). The α for the le Noble reaction coordinate has been shown[21a] to be quite similar to the Marcus α (eq 3b), one indication of the powerful generality of the Marcus equation. Additional evidence for this generality is found in other treatments,[26] which obtain the Marcus equation without assuming an explicit form for the potential or free energy function along the reaction coordinate. This work suggests that the Marcus treatment is only one member of a broad family of rate–equilibrium relationships. The question of how broad the generality of these relationships may be continues to be an active area of research,[26] but the list of successful applications grows steadily longer. In spite of the lack of rigorous theoretical justification for including gas-phase S_N2 reactions on this list, the kinetic–thermodynamic separation that is characteristic of these rate–equilibrium treatments is an extremely useful concept in interpretation of nucleophilic displacements. It is this general point that we wish to emphasize in our model; whether the Marcus equation correlates potential energy surfaces of S_N2 reactions better than other rate-equilibrium relations is of secondary concern, since differences between the treatments proposed to date tend to be small.[27] Marcus theory was chosen for use in our analysis because of its convenience and general familiarity rather than out of any quantitative preferences.

As is the case for all rate–equilibrium relationships of this type, eq 3 may be applied only to isolated elementary reactions. The chemically most important elementary step in the mechanism of Figure 1, and the one on which our analysis will focus, is the unimolecular complex-to-complex rearrangement shown in eq 2. The central barrier height determined with the RRKM-based method outlined above becomes $\Delta E^{\ddagger}$, and ΔE is the energy dif-

ference between the two complexes. In general this will be similar to the overall ΔE ($\approx \Delta H°$) between separated reactants and products, although corrections can be made[8] for those cases in which the reactant and product neutrals differ dramatically in structure. Inserting this $\Delta E^{\ddagger}$ and ΔE into eq 3a and solving for $\Delta E^{\ddagger}{}_0$ removes the thermodynamic contribution to $\Delta E^{\ddagger}$, leaving the purely kinetic intrinsic barrier. According to the additivity relation mentioned earlier, the intrinsic barrier is given by the mean of the barriers to the exchange processes shown in eq 4.

$$X^- \cdot CH_3X \rightarrow XCH_3 \cdot X^- \qquad \Delta E^{\ddagger}{}_0(4a) \qquad (4a)$$

$$Y^- \cdot CH_3Y \rightarrow YCH_3 \cdot Y^- \qquad \Delta E^{\ddagger}{}_0(4b) \qquad (4b)$$

$$X^- \cdot CH_3Y \rightarrow XCH_3 \cdot Y^- \qquad \Delta E^{\ddagger}{}_0(4c) \qquad (4c)$$

$$\Delta E^{\ddagger}{}_0(4c) = \tfrac{1}{2}[\Delta E^{\ddagger}{}_0(4a) + \Delta E^{\ddagger}{}_0(4b)] \qquad (4d)$$

The central barrier height for the chloride exchange in eq 5

$$^{37}Cl^- + CH_3{}^{35}Cl \rightarrow {}^{35}Cl^- + CH_3{}^{37}Cl \qquad (5)$$
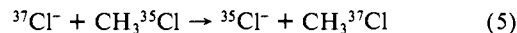
can be determined[8] by using the RRKM approach discussed above, since the rate constant has been measured.[7] The resulting barrier height is $\Delta E^{\ddagger}{}_0(Cl^- + CH_3Cl)$ because the reaction is thermoneutral. This quantity and eq 4 allow entry into a range of $\Delta E^{\ddagger}{}_0(X^- + CH_3X)$ if we study reactions of various nucleophiles X^- with methyl chloride. An analogous treatment of reactions of X^- with methyl bromide is also possible, although with larger uncertainties since the efficiency of the bromide exchange reaction can only be estimated.[7,8] Results of the Marcus calculations appear in Table III.

Discussion

The quantity $\Delta E^{\ddagger}{}_0(X^- + CH_3X)$, the height of the central barrier on this reaction's double-minimum potential surface, provides a useful framework for describing the intrinsic (solvent- and thermodynamics-free) nucleophilicity of X^- toward methyl centers. The Marcus treatment of S_N2 reactions renders nucleophilicity and leaving-group ability equivalent, since in the defining reaction X^- behaves both as nucleophile and leaving group. This "symmetry" has been pointed out previously.[5] Also, intrinsic nucleophilicities can be treated without arbitrarily chosen reference substrates or reference solvents, features that have been a problem in past treatments.

In our initial work, reactions of fluoride and alkoxides with methyl halides were interpreted by using this model. These cases were used to illustrate several of the model's important characteristics and consequences, which will not be repeated here. Table III also contains results for several additional nucleophiles that were studied subsequently. This group includes anions such as acetate and acetylide, which have not received a great deal of attention in study of solution-phase S_N2 reactions. Perhaps the most noteworthy feature of the systems in Table III is the range of ~30 kcal/mol in the exchange barriers. We now explore a model that can account for this wide variation. Before doing so, however, some comments are in order regarding uncertainties in our calculations.

As is evident in Table III, changes in input parameters of the RRKM calculations can lead to quite different values for $\Delta E^{\ddagger}{}_0$ in a given system. This is especially the case for the small polyatomic nucleophiles that react with efficiencies of ~10% or greater, where the range of values for $\Delta E^{\ddagger}{}_0$ can be as much as ±7 kcal/mol. This arises primarily from our lack of detailed information about the low-frequency modes in the k_2 transition state. Other sources of uncertainty include our assumptions regarding well depths, the treatment of internal rotations,[8] and the additivity relation in eq 4, although these factors are less important than that due to choice of frequency for low-frequency modes. However, for most of the calculations α lies in the range ~0.2–0.3; hence it is unlikely that the frequencies of these modes will vary greatly from system to system.[8] Thus, we feel justified in comparing intrinsic barriers for different nucleophiles obtained from calculations using the same set of values (for instance, 200 cm^{-1} in Table III) for the low-frequency modes. Although results

(18) Although the more common free-energy form of eq. (3) was used in our original work (ref. 8), we now believe that application of the potential energy form is more intuitive and straightforward.

(19) Weston, R. E.; Schwartz, H. A. "Chemical Kinetics"; Prentice-Hall: Englewood Cliffs, NJ, 1972; Section 7.7.

(20) (a) Cohen, A. D.; Marcus, R. A. *J. Phys. Chem.* **1968**, *72*, 4249. (b) Marcus, R. A. *J. Am. Chem. Soc.* **1969**, *91*, 7224. (c) Kreevoy, M. M.; Konasewitch, D. E. *Adv. Chem. Phys.* **1971**, *21*, 243. (d) Albery, W. J.; Campbell-Crawford, A. N.; Curran, J. S. *J. Chem. Soc., Perkins Trans. 2* **1972**, 2206. (e) Kreevoy, M. M.; Oh, S.-W. *J. Am. Chem. Soc.* **1973**, *95*, 4805. (f) Kresge, A. J. *Chem. Soc. Rev.* **1973**, *2*, 475. (g) Murdoch, J. R. *J. Am. Chem. Soc.* **1980**, *102*, 71.

(21) (a) Albery, W. J. *Pure Appl. Chem.* **1979**, *51*, 949. (b) Lewis, E. S.; Kukes, S. *J. Am. Chem. Soc.* **1979**, *101*, 417. (c) Lewis, E. S.; Kukes, S.; Slater, C. D. *Ibid.* **1980**, *102*, 1619.

(22) Magnoli, D. E.; Murdoch, J. R. *J. Am. Chem. Soc.* **1981**, *103*, 7465.

(23) Marcus, R. A. *Annu. Rev. Phys. Chem.* **1964**, *15*, 155 and references cited therein.

(24) Marcus, R. A. *Discuss. Faraday Soc.* **1960**, *29*, 21.

(25) le Noble, W. J.; Miller, A. R.; Hamann, S. D. *J. Org. Chem.* **1977**, *42*, 338.

(26) (a) Murdoch, J. R. *J. Am. Chem. Soc.* **1972**, *94*, 4410. (b) Agmon, N.; Levine, R. D. *Isr. J. Chem.* **1980**, *19*, 330. (c) Reference 22 and references cited therein.

(27) (a) Agmon, N. *J. Chem. Soc., Faraday Trans. 2* **1977**, *74*, 388. (b) Miller, A. R. *J. Am. Chem. Soc.* **1978**, *100*, 1984.
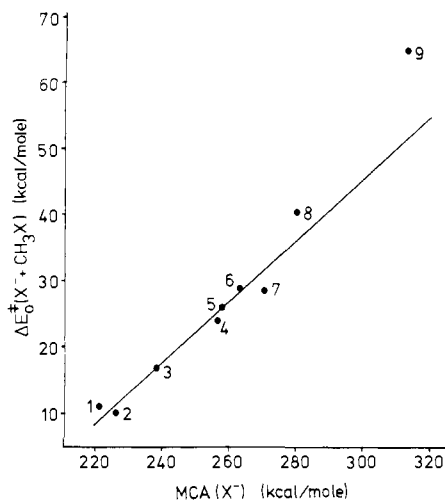
2676 *J. Am. Chem. Soc., Vol. 105, No. 9, 1983*

Pellerite and Brauman

Figure 2. Plot of $\Delta E^{*}_{0}(X^{-} + CH_{3}X)$ vs. MCA(X^{-}) for species in Table I. The straight line is the least-squares fit to the data, excluding point 9: (1) X = Br, (2) X = Cl, (3) X = CH$_{3}$CO$_{2}$, (4) X = CD$_{3}$S, (5) X = F, (6) X = *t*-BuO, (7) X = CH$_{3}$O, (8) X = HCC, (9) X = H (theoretical, ref 28).

from this treatment are only quantitatively accurate to within several kcal per mole, we believe that the accuracy is more than adequate to allow a qualitative picture to emerge.

A Structure–Reactivity Correlation for Gas-Phase S$_{N}$2 Reactions. The data in Table III immediately raise the question of why, for example, the barrier to acetylide exchange should be much larger than that to chloride exchange. These barriers are purely kinetic, since there is no thermodynamic driving force. Rationalizations such as "chloride is a better leaving group than acetylide" are simply restatements of the question and offer no physical insight.

The usual way of answering questions such as this one is to search for correlations with thermodynamic or spectroscopic quantities. With this approach one transfers responsibility for the observed effect to another property, but it can provide insight into the physical mechanism that produces the observed correlation.

In this case, it is not obvious that any thermodynamic property of the X^{-} + CH$_{3}$X system should correlate with the intrinsic barrier, since the latter is a purely kinetic property. Indeed, plots of $\Delta E^{*}_{0}(X^{-} + CH_{3}X)$ vs. X^{-} proton affinity, X$\cdot$electron affinity, and CH$_{3}$–X bond dissociation energy all yield poor correlations. However, Figure 2 shows the monotonic relationship that is observed when $\Delta E^{*}_{0}(X^{-} + CH_{3}X)$ obtained with the 200-cm^{-1} model (Table III) is plotted against the methyl cation affinity (MCA) of the nucleophile. MCA(X^{-}) is defined in eq 6 and is the
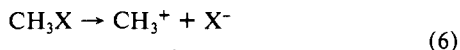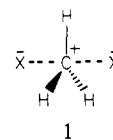
$$CH_{3}X \rightarrow CH_{3}^{+} + X^{-}$$
$$\Delta H^{\circ} = MCA(X^{-}) = D^{\circ}(CH_{3}\text{–}X) - EA(X) + IP(CH_{3}) \quad (6)$$

heterolytic bond dissociation energy of the CH$_{3}$–X bond. In this equation, EA(X) is the electron affinity of the X radical and IP(CH$_{3}$) is the methyl radical ionization potential. As seen in Figure 2, as the methyl cation affinity of the nucleophile X^{-} increases, so does the height of the intrinsic barrier to the exchange reaction X^{-}·CH$_{3}$X $\rightarrow$ XCH$_{3}$·X^{-}. This correlation also includes the calculated[28] exchange barrier for H^{-} + CH$_{4}$, although quantitatively the agreement is not perfect.

How is this observation to be interpreted? We believe the monotonic increase of $\Delta E^{*}_{0}(X^{-} + CH_{3}X)$ with X^{-} methyl cation affinity to be a consequence of charge separation in the trigonal-bipyramidal transition state of the exchange reaction. Theoretical calculations[29] have demonstrated substantial contributions

to S$_{N}$2 transition states by resonance structures of the form **1**, so

$$\bar{X} \text{---} \overset{\overset{\displaystyle H}{|}}{\underset{\overset{\displaystyle H}{H}}{\overset{\displaystyle +}{C}}} \text{---} \bar{X}$$

1

that passage from reactants X^{-}·CH$_{3}$X to the transition state and heterolytic cleavage of the CH$_{3}$–X bond both involve the same type of charge separation. Although we do not claim that the relationship must necessarily be linear (because the charge distribution in **1** surely depends on the structure of X), the slope of the least-squares line in Figure 2 is $\sim$0.5, which suggests incomplete charge development in the transition state. We note that some S$_{N}$2 reactions in solution show positive values of ρ but this may be a consequence of a tight transition state and substituent response to the net charge on the system.

Thus, within the framework of this model, acetylide is a much poorer nucleophile than chloride because acetylide's methyl cation affinity is larger than chloride's. One can carry this analysis a step further by using eq 6 and noting that the electron affinities of the two radicals are similar.[30] The difference in nucleophilicities is then seen to arise from the large difference in the CH$_{3}$–CCH and Cl–CH$_{3}$ homolytic bond dissociation energies. A similar treatment of methoxide and chloride shows that the much poorer nucleophilicity of methoxide may be traced to the electron affinity of methoxyl being lower than that of chlorine, since the homolytic CH$_{3}$–X bond dissociation energies are similar.[31]

An alternative interpretation of the correlation in Figure 2 is that it is an artifact of the RRKM calculations and Marcus analysis. The RRKM calculations reveal that the calculated efficiency is a quite-sensitive function of the energy gap $\Delta E'$ between the two transition states. This effect was observed in calculations on all of the different reactions. The dynamic range of pulsed ICR is such that only reactions with efficiencies greater than $\sim$10^{-3} are observable. This narrow range of experimentally accessible efficiencies coupled with the sensitivity of calculated efficiency to small changes in $\Delta E'$ means that central barrier heights determined by this method are always within $\sim$8 kcal/mol or so of each other. This is small compared to the range of ΔH°'s in Table I. If one now takes a series of reactions having similar barriers but varying exothermicities and uses the Marcus equation to solve for their intrinsic barriers, it will turn out that the most exothermic reaction will have the largest intrinsic barrier. Furthermore, methyl cation affinity is directly related to exothermicity, as shown in eq 7. Since experimental considerations have limited

$$A^{-} + CH_{3}B \rightarrow B^{-} + CH_{3}A$$
$$\Delta H^{\circ} = MCA(B^{-}) - MCA(A^{-}) \quad (7)$$
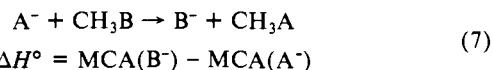
us to only two substrates (CH$_{3}$Cl and CH$_{3}$Br), both of which appear to have similar intrinsic barriers to nucleophilic exchange, all of these factors could combine to produce a correlation between $\Delta E^{*}_{0}(X^{-} + CH_{3}X)$ and MCA(X^{-}), which is totally unrelated to any physical mechanism.

It is doubtful that this interpretation is correct. As shown below, the intrinsic barriers in Table III have considerable predictive power in terms of which reactions should proceed quickly and which should be too slow to measure with available methods. The observation that the calculated[28] barrier to the H^{-} + CH$_{4}$ exchange fits at least qualitatively on the plot in Figure 2 provides some additional evidence that the intrinsic barriers in Table III are physically real, significant quantities and not merely artifacts of the analysis used to calculate them.

Finally, we note that although this type of correlation is unprecedented for S$_{N}$2 reactions, an analogous correlation between intrinsic barrier to exchange and base proton affinity has been

(28) Leforestier, C. *J. Chem. Phys.* **1978**, *68*, 4406 and references cited therein.

(29) (a) Dedieu, A.; Veillard, A. *J. Am. Chem. Soc.* **1972**, *94*, 6730. (b) Bader, R. F. W.; Duke, A. J.; Messer, R. R. *Ibid.* **1973**, *95*, 7715.

(30) (a) EA(Cl) = 3.61 eV: Hotop, H.; Lineberger, W. C. *J. Phys. Chem. Ref. Data* **1975**, *4*, 539. (b) EA(HCC) = 2.94 eV: Janousek, B. K.; Brauman, J. I.; Simons, J. *J. Chem. Phys.* **1979**, *71*, 2057.

(31) D°(CH$_{3}$–Cl) = 83.6, D°(CH$_{3}$–OCH$_{3}$) = 81.4 kcal/mol: Egger, K. W.; Cocks, A. T. *Helv. Chim. Acta* **1973**, *56*, 1516.

Table IV. S_N2 Reactions with Observed Efficiencies below Detection Limits[a] in Accord with Prediction

reaction	method,[b] reference	$\Delta H°$,[c] kcal/mol
Exchange Reactions		
$D^- + CH_4 \rightarrow H^- + CH_3D$	FA[d]	~0
$CD_3O^- + CH_3OCH_3 \rightarrow CH_3O^- + CD_3OCH_3$	ICR[e]	~0
$CD_3S^- + CH_3SCH_3 \rightarrow CH_3S^- + CD_3SCH_3$	ICR[f]	~0
Cross-Reactions		
$t\text{-BuO}^- + CH_3F \rightarrow F^- + t\text{-BuOCH}_3$	ICR[f]	−7
$HCC^- + CH_3F \rightarrow F^- + HCCCH_3$	FA[g]	−24
$CN^- + CH_3F \rightarrow F^- + CH_3CN$	FA[g]	−5
$OH^- + CH_3OCH_3 \rightarrow CH_3O^- + CH_3OH$	FA[h]	−6
$NH_2^- + CH_3OCH_3 \rightarrow CH_3O^- + CH_3NH_2$	FA[h]	−19

[a] Detection limits: Eff ~10^{-4} (FA), ~10^{-3} (ICR). [b] FA = flowing afterglow, ICR = ion cyclotron resonance. [c] Calculated with data from ref 52 and 53. [d] Reference 54. [e] Reference 7. [f] This work. [g] Reference 37. [h] Reference 39.

proposed on theoretical grounds for proton transfers.[32]

Supporting Evidence for the Model. Two types of evidence are discussed here that support the Marcus treatment of gas-phase S_N2 reactions. The first is experimental confirmation of predictions made by the model regarding rates of several S_N2 reactions, while the second type is purely theoretical.

1. Predictions Regarding Exchange Reactions. Given that the lowest ion–molecule reaction efficiency measurable by current methods is ~10^{-4} (by flowing afterglow[33]), the RRKM calculations show that any S_N2 reaction with a central barrier larger than ~12 kcal/mol (assuming a 10 kcal/mol well depth) should be too slow to observe. Thus, all of the self-exchange reactions of X and Y in Table III except for those involving Cl^- and Br^- exchange (which were used to determine the others) should be far too slow to measure. Some of these predictions have been verified experimentally, in addition to the methoxide exchange[7] discussed earlier.[8] These are shown in Table IV. Of particular interest is the CH_3S^- exchange. Our results on this system show that CH_3S^- behaves normally in terms of the plot in Figure 2 and that its reaction with CH_3SCH_3 is extremely slow as predicted. However, the similar reaction in eq 8 has been reported[7,34] to

$$CH_3S^- + CH_3SH \rightarrow SH^- + CH_3SCH_3 \quad (8)$$
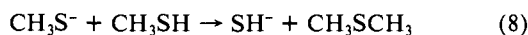
proceed fairly readily with an efficiency of 0.05. Although this reaction is 8 kcal/mol exothermic, use of our intrinsic barrier for CH_3S^- exchange along with the assumption that the SH^- exchange barrier is similar leads the Marcus model to predict that the reaction should be extremely slow. This is in accord with work of Mackay and Bohme.[35] We are thus forced to attribute our earlier observation of reaction 8 to either H_2S impurity or a filament reaction. Also, the normal behavior of CH_3S^- in the gas phase indicates that the enhanced reactivity of alkyl thiolates and other sulfur nucleophiles in solution[36] is a solvation phenomenon.

2. Predictions Regarding Cross-Reactions. One useful feature of the Marcus treatment is that given intrinsic barriers for a series of exchange reactions, the additivity relation and the Marcus equation allow barriers to cross-reactions to be calculated provided the necessary thermodynamics are known. At this point, this is not a useful method for estimating efficiencies for S_N2 reactions, since as we have seen, the RRKM calculated efficiency is quite sensitive to barrier height and our calculations are not of sufficient precision. However, we can again predict which cross-reactions

will have central barriers so large as to render them immeasurably slow. Table IV shows the cases that have been confirmed experimentally.

The reaction of HCC^- with CH_3F is particularly interesting, as it is substantially exothermic yet proceeds slowly, if at all. Although we have not dealt with OH^- or NH_2^- in our model, their reactions with CH_3OCH_3 are included in Table IV because they support our earlier statement[8] that displacement of CH_3O^- from CH_3OCH_3 should be extremely slow even when exothermic. In fact, NH_2^- and OH^- react with alkyl ethers exclusively by β-elimination;[38] the small amounts of S_N2 products that are observed in reactions of ethers without β-hydrogens can be attributed to the presence of impurities, as experiments with highly purified ether[39] showed that reaction between OH^- and CH_3OCH_3 is imperceptibly slow and produces no CH_3O^-.

To our knowledge, the only piece of data currently in the literature that is at odds with our predictions regarding the nucleophiles studied here is the observation by Bohme and co-workers[37] that CH_3O^- reacts with CH_3F with an efficiency of 0.007. We believe this result may also have arisen from impurities, as our efforts to detect reaction between $t\text{-BuO}^-$ and CH_3F by ICR failed to produce any F^- signal.[40] This observation is in agreement with our model's prediction.

However, we do not mean to imply that all F^- displacements from CH_3F must be immeasurably slow, although this is the case for the nucleophiles studied here. Whereas our data predict $\Delta E^* = 20$ kcal/mol for $CH_3O^- + CH_3F$, use of $\Delta E^*_0(H^- + CH_4) = 51$ kcal/mol obtained from the line in Figure 2 leads to $\Delta E^* = 15$ kcal/mol for $H^- + CH_3F$. This value is getting into the range where reaction of a light, monatomic nucleophile could possibly proceed slowly. Thus, we can make no definite predictions regarding this reaction and would not rule out the possibility that it may proceed with low efficiency.

With this in mind, it is interesting to note that Bohme and co-workers[37] have reported an efficiency of 0.002 for the reaction of H^- with CH_3F. However, several other species such as OH^- and NH_2^- are also reported to react slowly but measurably with CH_3F to produce F^-. Treatment of OH^- and NH_2^- in a manner analogous to that described above for H^- leads us to predict that, like CH_3O^-, their reactions with CH_3F should be undetectable. Observation of these reactions, including that of H^-, may also arise from impurities. And, the possibility of some additional stabilizing interaction (such as H bonding) involving highly basic nucleophiles such as OH^- and NH_2^-, which lowers the energies of both complex and S_N2 transition state relative to separated reactants, cannot be ruled out (see next section). At this point we cannot assess these alternatives.

In spite of these uncertainties, it is important to note that, in general, S_N2 reactions with CH_3F are at the very least much slower than reactions with CH_3Cl and CH_3Br of comparable exothermicities; this trend is predicted by our model.

3. Theoretical Support. As mentioned in our earlier work,[8] several sets of ab initio quantum mechanical calculations[29,41] have verified the general form of the double-minimum potential surface for gas-phase S_N2 reactions; the calculated central barrier height for fluoride exchange was in reasonable agreement with that determined from our procedure. Also, we have seen that the calculated barrier for hydride exchange fits fairly well on our plot of $\Delta E^*_0(X^- + CH_3X)$ vs. MCA(X^-) in Figure 2 and shows that our prediction of exchange barriers in excess of 30 kcal/mol for some species is physically reasonable.

Work of Wolfe, Mitchell, and Schlegel[42] appeared recently in which our proposal of a rate-equilibrium treatment of S_N2 reactions was tested theoretically. Their approach was to calculate

(32) Murdoch, J. R.; Magnoli, D. E. *J. Am. Chem. Soc.* **1982**, *104*, 3792.

(33) DePuy, C. H.; Bierbaum, V. M. *Acc. Chem. Res.* **1981**, *14*, 146.

(34) (a) Lieder, C. A. Ph.D. Thesis, Stanford University, 1974. (b) Table I in ref 7 contains a misprint in the reported efficiency of reaction 8.

(35) Mackay, G. I.; Bohme, D. K. *Int. J. Mass Spectrom. Ion Phys.* **1978**, *26*, 327.

(36) Hartshorn, S. R. "Aliphatic Nucleophilic Substitution"; Cambridge University Press: London, 1973; p 45 ff.

(37) Tanaka, K.; Mackay, G. I.; Payzant, J. D.; Bohme, D. K. *Can. J. Chem.* **1976**, *54*, 1643.

(38) DePuy, C. H.; Bierbaum, V. M. *J. Am. Chem. Soc.* **1981**, *103*, 5034.

(39) Bierbaum, V. M., personal communication.

(40) In our hands, reaction with an unknown impurity in the CH_3F samples aborted efforts to verify Bohme's result for $CH_3O^- + CH_3F$.

(41) (a) Dedieu, A.; Veillard, A. *Chem. Phys. Lett.* **1970**, *5*, 328. (b) Keil, F.; Ahlrichs, R. *J. Am. Chem. Soc.* **1976**, *98*, 4787. (c) Schlegel, H. B.; Mislow, K.; Bernardi, F.; Bottini, A. *Theor. Chim. Acta* **1977**, *44*, 245.

(42) Wolfe, S.; Mitchell, D. J.; Schlegel, H. B. *J. Am. Chem. Soc.* **1981**, *103*, 7694.

Table V. Comparison of Experimental and Theoretical Values for $\Delta E^{\ddagger}_0(X^- + CH_3X)$

	$\Delta E^{\ddagger}_0(X^- + CH_3X)$, kcal/mol	
X	experimental[a]	theoretical[b]
HCC	41.3	50.4
CN[c]	35.0[d]	43.8
CH$_3$O	26.6	23.5
CH$_3$S[e]	24.2	15.6
F	26.2	11.7
Cl	10.2	5.5

[a] This work. [b] Calculations of Wolfe et al.[42] [c] Assuming C-alkylation. [d] See Discussion. [e] Calculated value is $\Delta E^{\ddagger}_0(HS^- + CH_3SH)$.

central barrier heights for cross-reactions $X^- + CH_3Y \rightarrow Y^- + CH_3X$ involving various nucleophiles X and Y, calculate the exchange barriers $\Delta E^{\ddagger}_0(X^- + CH_3X)$ and $\Delta E^{\ddagger}_0(Y^- + CH_3Y)$, and then see if the results are consistent with the Marcus equation. In all cases the internal consistence was excellent, indicating that the potential surfaces are indeed correlated by the Marcus expression.

Table V compares intrinsic barriers determined by Wolfe et al. and by our procedure for nucleophiles common to both treatments; agreement ranges from excellent to poor. Also the intrinsic barrier–methyl cation affinity correlation is not followed rigorously in Wolfe's work. At this point there is little to be gained in speculating over which treatment is superior. In spite of these differences, the application of Marcus theory represents a major step forward in the understanding of structure–reactivity relationships in S_N2 reactions.

Several aspects of Wolfe's work deserve comment. First, calculated well depths for encounter complex formation with a fixed substrate are seen to vary widely with ion structure. For instance, the $X^-\cdot CH_3F$ well depth goes from 12 kcal/mol with X = CN (overall $\Delta H^\circ = -5$ kcal/mol) to 23 kcal/mol with X = OH (overall $\Delta H^\circ = -19$ kcal/mol). Since displacements from CH$_3$F are all extremely slow, these figures are amenable to experimental verification. If correct, they would indicate that there may indeed be significant bonding in the complexes, meaning that the well depth may be influenced by the overall reaction thermodynamics or perhaps by hydrogen bonding involving strongly basic localized nucleophiles such as OH$^-$. This type of effect could be responsible for the reported[37] occurrence of several reactions of CH$_3$F discussed earlier. However, there is some reason to question these calculations. According to our RRKM calculations, if Wolfe's calculated $\Delta E'$ (Figure 1) of 13 kcal/mol for OH$^- + CH_3F$ were correct, the reaction efficiency would be nearly unity, much larger than observed.[37] Thus, we await experimental evidence before abandoning our assumptions concerning well depths for ion–molecule complexes and their dependence (or lack of) on ion structure.[43] Also, among the species in Table V the largest disagreement between the experimental and theoretical results occurs for F$^-$, for which this calculated $\Delta E^{\ddagger}_0(F^- + CH_3F)$ is significantly smaller than earlier values.[8] Our result is in much better agreement with the older work.

In the meantime, these calculations along with evidence discussed earlier serve to demonstrate the validity of our Marcus model of reactivity in gas-phase S_N2 reactions, although as we have seen many quantitative details remain to be worked out.

Very recently, Shaik and Pross have presented a theoretical treatment of S_N2 reactions based on a valence bond approach.[44]

In this picture,[44a] the barrier arises from an avoided crossing involving donor–acceptor states. The model shows generally good qualitative agreement with our experimental results. It will be interesting to explore the quantitative relationship between the Shaik–Pross surface crossing and our empirical correlation with methyl cation affinity as well as comparing reactions of delocalized nucleophiles (see below).

It should be noted that the gas-phase barriers that Shaik and Pross have derived from experimental data appear to have been computed with the assumption[44a] that $\Delta E_2^{\ddagger} - \Delta E_1^{\ddagger} = \ln (k_1/k_2)$. We have pointed out in our previous work[7,8] as well as in this one that there is no simple relationship that connects the observed rate constant with even the energy (height) of the top of the barrier. In addition, the well depth has no effect on the reaction efficiency so that the barrier height, $E^{\ddagger}$, cannot be obtained without further information about the well depth. However, the "experimental" barriers derived by Shaik and Pross agree with ours to within several kcal/mol probably because of other factors,[44e] and the general conclusions drawn from their model are presumably not affected.

Reactions of Delocalized Nucleophiles. One of the factors believed to be important in determining intrinsic barrier heights in transfer reactions is the extent of structural reorganization that occurs upon passage from reactants to transition state. The larger the structural change, the larger the intrinsic barrier. This can be illustrated by considering a proton exchange between an acid AH and its delocalized conjugate base A$^-$. In the symmetrical transition state for this process, both A fragments must be distorted away from their equilibrium geometries; this bond reorganization costs energy and thus leads to a larger barrier than in a case involving proton transfer between localized bases whose structures do not change greatly upon protonation.

This effect may appear in S_N2 reactions in the form of an increase in the intrinsic barrier $\Delta E^{\ddagger}_0(X^- + CH_3X)$ relative to that for a localized nucleophile of comparable methyl cation affinity. The possibility that delocalization could affect reactivity in displacement reactions has been raised by Bohme and Young,[45] although their analysis was purely qualitative. The model we have proposed here for gas-phase S_N2 reactions allows us to study delocalization effects quantitatively by determining $\Delta E^{\ddagger}_0(X^- + CH_3X)$ for the delocalized nucleophile using the procedure outlined above and then placing this point on the plot in Figure 2. The vertical displacement of the point above the line is then indicative of the contribution of delocalization to $\Delta E^{\ddagger}_0(X^- + CH_3X)$ for our delocalized nucleophile, if one assumes that the line describes behavior of "normal", localized species.

One troublesome feature of many delocalized nucleophiles is that their alkylations can yield more than one possible neutral product. Although this is unlikely for some of the species we have studied, it is a distinct possibility for others and introduces an element of ambiguity into the analysis. For these latter cases, we have applied the Marcus model to each available pathway. However, it is hoped that these problems will soon be resolved by using techniques that have been developed recently[46] for detection and identification of neutral products from ion–molecule reactions.

Table II shows the delocalized nucleophiles we have examined as well as data for additional species taken from other work. The last three entries are systems for which only upper limits to the rate constants could be obtained; these were not considered further. RRKM and Marcus calculations for the other reactions in Table II were performed by using the procedures given earlier. In these cases the uncertainty in the calculations is greater than for those discussed earlier, since some of these delocalized anions are strongly asymmetric tops. This introduces another approximation in the treatment of internal rotations in the k_{-1} transition state.[8] In all cases, results from the 200-cm^{-1} model were used to compare

(43) See, for some values: Kebarle, P. *Annu. Rev. Phys. Chem.* **1977**, *28*, 445.

(44) (a) Shaik, S. S.; Pross, A. *J. Am. Chem. Soc.* **1982**, *104*, 2708. (b) Also see: Shaik, S. S. *Nouv. J. Chim.* **1982**, *6*, 159. (c) Pross, A.; Shaik, S. S. *J. Am. Chem. Soc.* **1982**, *104*, 1129. (d) Shaik, S. S. *Ibid.* **1981**, *103*, 3692. (e) Notwithstanding an omitted *RT*, "calibrating" the calculations to $\Delta E^{\ddagger}$ and *k* ensures that $RT \ln (k_1/k_2)$ will be ~±3 kcal/mol or less and the central barriers will be similar to ours. As mentioned (see Discussion) the order of intrinsic barriers can be reproduced with the Marcus expression and a single $\Delta E^{\ddagger}$. Thus, agreement with our observed trends does not constitute a justification of the Shaik–Pross assumption.

(45) Bohme, D. K.; Young, L. B. *J. Am. Chem. Soc.* **1970**, *92*, 7354.

(46) (a) Lieder, C. A.; Brauman, J. I. *Int. J. Mass Spectrom. Ion Phys.* **1975**, *16*, 307; (b) *J. Am. Chem. Soc.* **1974**, *96*, 4028. (c) Burns, F. B.; Morton, T. H. *Ibid.* **1976**, *98*, 7308. (d) Smith, M. A.; Barkley, R. M.; Ellison, G. B. *Ibid.* **1980**, *102*, 6851.
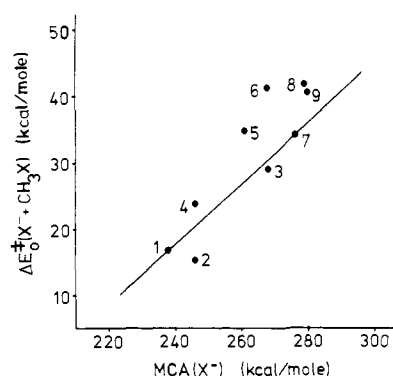
Intrinsic Barriers in Nucleophilic Displacements

J. Am. Chem. Soc., Vol. 105, No. 9, 1983 2679

Figure 3. Plot of $\Delta E^{*}_{0}(X^{-} + CH_{3}H)$ vs. $MCA(X^{-})$ for delocalized nucleophiles in Table V. The straight line is that from Figure 2: (1) X = $CH_{3}CO_{2}$, (2) X = $CH_{3}COCH_{2}$ (O-alkylation), (3) X = $CH_{3}COCH_{2}$ (C-alkylation), (4) X = CN (N-alkylation), (5) X = CN (C-alkylation), (6) X = PhN, (7) X = $CH_{2}CN$, (8) X = $PhCH_{2}$, (9) X = HCC.

with the plot in Figure 2. Also, the assumption made previously regarding reactant complex well depth was used in these calculations.

Results of these efforts appear in Figure 3, in which values of $\Delta E^{*}_{0}(X^{-} + CH_{3}X)$ are shown superimposed on the line from Figure 2. Overall, there appears to be little consistent effect of delocalization on reactivity for these systems, within the framework of this model. Phenylnitrene radical anion, $PhN^{-}\cdot$, is the only species that shows any significant effect (~ 10 kcal/mol), and even this may be an artifact given that benzyl anion, $PhCH_{2}^{-}$, seems to behave normally. In fact, the barriers for HCC^{-} exchange and $PhCH_{2}^{-}$ exchange are essentially identical. There is no obvious reason why $PhN^{-}\cdot$ should show a delocalization effect while $PhCH_{2}^{-}$, which is probably the more delocalized of the pair, is quantitatively similar in behavior to the predominantly localized HCC^{-}. The RRKM calculations on $PhCH_{2}^{-}$ methylation indicate that this reaction is slow for entropic reasons. This ion has the largest moments of inertia of any species we have investigated, and hence more internal rotational entropy is lost upon attaining the tight $S_{N}2$ transition state than for small species such as $CH_{3}O^{-}$ or HCC^{-}. Consequently, only comparatively small barriers are required to produce low efficiencies, and hence the low efficiency for $PhCH_{2}^{-}$ methylation is not reflected as an increase in the intrinsic barrier to $S_{N}2$ exchange relative to those for smaller, localized nucleophiles. For this reason, one must exercise caution when using reaction efficiencies to gain insight into relative reactivities.

Thus, within the framework of this model, there appears to be no significant difference in reactivity (as measured by the intrinsic barriers) between the localized and delocalized nucleophiles among the systems studied. One reason for this behavior may be that these anions simply do not undergo large enough structural change, upon proceeding from anion to $S_{N}2$ transition state to methylated product, to induce detectable deviation from "normal", localized behavior by the intrinsic barriers $\Delta E^{*}_{0}(X^{-} + CH_{3}X)$. If this were the case, highly delocalized nucleophiles such as cyclopentadienyl anion might be expected to show larger effects. (A rate constant for reaction of this anion with methyl bromide has been reported recently,[47] but we have not used this value to obtain $\Delta E^{*}_{0}(C-C_{5}H_{5}^{-} + CH_{3}C_{5}H_{5})$.) Another possibility is that the depressed reactivity often shown by delocalized species in solution is related to solvation of the reactant, which suffers more reorganization when the charge is initially delocalized away from the reactive center.

Summary and Conclusions

In this paper we have used RRKM calculations and the double-minimum potential surface to estimate central barrier heights for several gas-phase nucleophilic displacement reactions. We

further propose that Marcus theory may be used to correlate these barrier heights with the thermodynamics of complex-to-complex rearrangement. The intrinsic barriers, $\Delta E^{*}_{0}(X^{-} + CH_{3}X)$, which are obtained from this analysis, form a useful framework within which to discuss intrinsic nucleophilicities of a wide range of species toward methyl centers.

Our treatment displays several attractive features. Defining intrinsic nucleophilicity in this fashion emphasizes the symmetry of the reaction, eliminating any need to distinguish between nucleophilicity and leaving-group ability. Also, since the reactions are studied in the dilute gas phase, solvent effects are absent and we can easily apply the Marcus expression to the appropriate elementary step. Finally, the model achieves the necessary separation of kinetic and thermodynamic contributions to reaction barriers, with the interesting result that many species generally considered "good" nucleophiles are predicted to be quite poor kinetically; their reactivity can thus be attributed to highly favorable overall thermodynamics. On this basis we also conclude that the poor leaving-group ability observed for species such as alkoxides in solution-phase $S_{N}2$ reactions is at least in part an intrinsic effect and not due solely to solvation, as this behavior persists when solvent is removed.

We observe a monotonic correlation between intrinsic nucleophilicity $\Delta E^{*}_{0}(X^{-} + CH_{3}X)$ and X^{-} methyl cation affinity, rationalized by charge separation in the $S_{N}2$ transition state which renders the processes described by the two quantities formally analogous. One application of this correlation is in the study of delocalization effects on anion nucleophilicity, although our initial efforts with several systems failed to reveal any major impact of delocalization on $\Delta E^{*}_{0}(X^{-} + CH_{3}X)$.

Support for our model is found in two forms: verification of predictions regarding reactions that are too slow for measurement by current techniques, and quantum mechanical calculations. Both indicate thus far that our treatment is at least qualitatively and possibly semiquantitatively correct. One cautionary note, however: at this point the model is not useful for predicting absolute rate constants, as the uncertainty in our intrinsic barrier calculations is at least several kcal per mole and the RRKM calculated efficiency is quite sensitive to central barrier height over the range generally encountered.

Finally, we note that barriers to methyl group exchange seem to be much larger than those to proton exchange. One example appears in eq 9. Proton transfer between methoxide and methanol

$$CD_{3}O^{-} + CH_{3}OH \rightarrow CD_{3}OH + CH_{3}O^{-} \qquad (9a)$$

$$CD_{3}O^{-} + CH_{3}OCH_{3} \rightarrow CD_{3}OCH_{3} + CH_{3}O^{-} \qquad (9b)$$

proceeds[48] with an efficiency close to 0.5, while that for the methyl transfer is over 4 orders of magnitude less.[7] Although there are certainly well-depth differences in these cases due to hydrogen bonding to methanol (~ 25 kcal/mol[49] for eq 9a vs. an estimated 10 kcal/mol for 9b), the central barrier (if any) to proton transfer must be small since the efficiency is close to the theoretical maximum. An analogous situation is also found in free radical chemistry. While activation energies for thermoneutral hydrogen-atom transfers are generally[50] 8–15 kcal/mol, a methyl-group transfer between two free radicals has yet to be observed even when exothermic.[51] Thus, the anionic and neutral reactions seem to be fundamentally linked. Whether the larger barriers to methyl transfer arise from electron correlation problems is still a matter

(47) McDonald, R. N.; Chowdhury, A. K.; Setser, D. W. *J. Am. Chem. Soc.* **1981**, *103*, 7586.

(48) Reference 34, p 192.
(49) Yamdagni, R.; Kebarle, P. *J. Am. Chem. Soc.* **1971**, *93*, 7139.
(50) Kerr, J. A. In "Comprehensive Chemical Kinetics"; Bamford, C. H., Tipper, C. F. H., Eds.; Elsevier: Amsterdam, 1977; Vol. 18, Chapter 2.
(51) Ingold, K. U.; Roberts, B. P. "Free-Radical Substitution Reactions"; Wiley-Interscience: New York, 1971; Chapter 5.
(52) Benson, S. W. "Thermochemical Kinetics", 2nd ed.; Wiley-Interscience: New York, 1976.
(53) Bartmess, J. E.; McIver, R. T., Jr. In "Gas-Phase Ion Chemistry"; Bowers, M. T., Ed.; Academic Press: New York, 1979; Vol. 2, Chapter 11.
(54) Payzant, J. D.; Tanaka, K.; Betowski, L. D.; Bohme, D. K. *J. Am. Chem. Soc.* **1976**, *98*, 894.

for speculation, although this seems to be a reasonable interpretation.

Acknowledgment. We are grateful to the donors of the Petroleum Research Fund, administered by the American Chemical Society, and to the National Science Foundation for support of this research and Fellowship support to M.J.P. We also thank Professors J. R. Murdoch and S. S. Shaik for sharing some unpublished results with us.

Orthoquinone Complexes of Vanadium and Their Reactions with Molecular Oxygen

Marion E. Cass, David L. Greene, Robert M. Buchanan, and Cortlandt G. Pierpont*
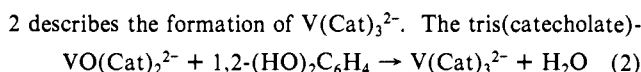
Contribution from the Department of Chemistry, University of Colorado, Boulder, Colorado 80309. Received September 10, 1982

Abstract: Reactions carried out between V(CO)₆ with 3,5-di-*tert*-butyl-1,2-benzoquinone and VO(acac)₂ with 3,5-di-*tert*-butylcatechol have been found to give as a common product V(3,5-DBSQ)₃. The V(CO)₆ reaction has been followed with EPR spectroscopy. Prior to observation of the 10-line radical spectrum of V(3,5-DBSQ)₃, an 8-line vanadium spectrum is observed that appears related to a mixed quinone–carbonyl species. The reaction between V(3,5-DBSQ)₃ and molecular oxygen has been followed, and the product [VO(3,5-DBSQ)(3,5-DBCat)]₂ has been characterized structurally. It crystallizes in the triclinic space group $P\bar{1}$ in a unit cell of dimensions $a = 11.486$ (4) Å, $b = 11.633$ (4) Å, $c = 13.102$ (4) Å, $\alpha = 100.58$ (2)°, $\beta = 108.81$ (3)°, $\gamma = 97.82$ (3)°, and $V = 1592.7$ (9) Å³. The dimeric molecule is located about a crystallographic center of inversion. Catecholate ligands bridge adjacent vanadium(V) ions through one oxygen; semiquinone ligands are chelated to the metals. Terminal oxo ligands bond at the sixth coordination sites of the metals. The complex exhibits an EPR spectrum which is that of a semiquinone coupled weakly with one vanadium (2.85 G) center. Further reaction with molecular oxygen gives V₂O₅ and the benzoquinone. Features of this reaction sequence are compared with related members of the series synthesized previously with molybdenum.

The chemistry of reactions carried out between vanadium ions of various charge and catechol has been a subject of interest for several years. Catechols were investigated as analytical agents for use in the photometric determination of vanadium.[1] This procedure took advantage of the intense charge-transfer bands associated with high-oxidation-state vanadium complexes formed with catecholate ligands. Recent work has been related to the biological activity of vanadium[2] and to application of the strong reducing power of vanadium(II)–catechol systems to the reduction of N₂ to ammonia, CO to methanol, and acetylenes to olefins.[3,4] Early experiments directed at understanding the chemistry of vanadium–catechol systems were carried out in protic media and appeared to give contradictory results. Within the past few years reports have appeared that focus on the pH dependence of these reactions, studies that have provided detailed characterization of reaction products.[5,6] Reactions carried out with vanadyl ion can be represented in two chemical equations. Equation 1 gives

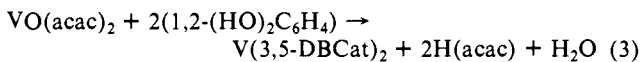$$VO^{2+} + 2(1,2\text{-}(HO)_2C_6H_4) \rightarrow VO(Cat)_2{}^{2-} + 4H^+ \quad (1)$$
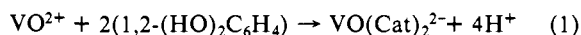
VO(Cat)₂²⁻ ion as the reaction product. A neutral VO(Cat) species that appears as an intermediate in the stepwise formation of the dianion has been isolated and characterized.[6,7] Equation 2 describes the formation of V(Cat)₃²⁻. The tris(catecholate)-

$$VO(Cat)_2{}^{2-} + 1,2\text{-}(HO)_2C_6H_4 \rightarrow V(Cat)_3{}^{2-} + H_2O \quad (2)$$

vanadium(IV) dianion can be either reduced or oxidized to give the vanadium(III) or vanadium(V) forms of the complex.[6,8]

A report by Wilshire and Sawyer concerning the reversible addition of O₂, NO, and CO to a vanadium(IV) complex prepared with 3,5-di-*tert*-butylcatechol (3,5-DBCat) was of considerable interest to us and other groups for its potential relationship to the gas-molecule reduction reactions discussed above.[9] Subsequent attempts to prepare the subject complex of this work, V(3,5-DBCat)₂, by the groups of both Raymond[6] and Sawyer[8] have failed. The reaction described in the initial report by Wilshire and Sawyer used vanadyl acetylacetonate as a reagent with the reaction carried out either in methanol or Me₂SO in the absence of additional acid or base (eq 3). Reactions described by Raymond and Sawyer in their recent reports were carried out under

$$VO(acac)_2 + 2(1,2\text{-}(HO)_2C_6H_4) \rightarrow$$
$$V(3,5\text{-}DBCat)_2 + 2H(acac) + H_2O \quad (3)$$

basic conditions and produced VO(3,5-DBCat)₂²⁻ ion as the product by the process described in reaction 1.

An alternate route to catecholate or, more generally, quinone complexes employs a reduced form of the metal and the oxidized form of the quinone ligand. We have used this approach with a wide variety of metals and have shown that in many cases the same products are obtained by this procedure as are obtained when using the oxidized metal–catechol route. A specific example that is pertinent to the work described in this report is found with

(1) Nardillo, A. M.; Catoggio, J. A. *Anal. Chim. Acta* **1975**, *74*, 85–99.
(2) Cantley, L. C.; Ferguson, J. H.; Kustin, K. *J. Am. Chem. Soc.* **1978**, *100*, 5210–5212.
(3) (a) Luneva, N. P.; Nikonova, L. A.; Shilov, A. E. *Kinet. Katal.* **1980**, *21*, 1458–1467. (b) Isalva, S. A.; Nikonova, L. A.; Shilov, A. E. *Nouv. J. Chim.* **1981**, *5*, 21–25.
(4) Schrauzer, G. N.; Palmer, M. R. *J. Am. Chem. Soc.* **1981**, *103*, 2659–2667.
(5) Henry, R. P.; Mitchell, P. C. H.; Prue, J. E. *J. Chem. Soc. Dalton Trans.* **1973**, 1156–1159.
(6) Cooper, S. R.; Koh, Y. G.; Raymond, K. N. *J. Am. Chem. Soc.* **1982**, *104*, 5092–5102.

(7) Wüthrich, K. *Helv. Chim. Acta* **1965**, *48*, 1012–1017.
(8) Bosserman, P. J.; Sawyer, D. T. *Inorg. Chem.* **1982**, *21*, 1545–1551.
(9) Wilshire, J. P.; Sawyer, D. T. *J. Am. Chem. Soc.* **1978**, *100*, 3972–3973.